Mössbauer measurements of static critical behavior in disordered *Fe*Al alloys

Gary Scott Collins, Ataur R. Chowdhury, and Christoph Hohenemser
Department of Physics, Clark University, Worcester, Massachusetts 01610
(Received 7 June 1982)

Mössbauer measurements were made on disordered $Fe_{1-x}Al_x$ alloys over the range $0 \leq x \leq 0.04$ in order to determine the critical exponent β. It was found, in agreement with theoretical predictions, that β remains unchanged with the addition of disorder. With the use of analysis that contains correction to scaling terms, a mean value of $\beta = 0.366(2)$ was found for five measurements. This is in excellent agreement with the renormalization-group prediction of $\beta = 0.365(1)$. A model was developed to help interpret critical behavior in the presence of a small distribution of critical temperatures observed in the alloy measurements.

I. INTRODUCTION

Over the past decade the renormalization-group (RG) approach has been highly successful in describing critical behavior at second-order phase transitions. For pure systems the theory predicts that static critical exponents depend only on order parameter dimensionality n and lattice dimensionality d. For disordered systems predictions are more varied and depend on the type of disorder (site versus bond), its statistical distribution (quenched versus annealed), and on the sign of the specific heat exponent α_p in the pure system.

For quenched disorder exact calculations for $d=2$ indicate[1,2] that the transition will be smeared or sharp depending on the statistical distribution of the disorder. For systems of arbitrary dimensionality, Harris[3] has shown that a sharp transition *can* exist in the presence of quenched, randomly placed impurities, but only if the pure system has a specific heat exponent $\alpha_p < 0$. Since the work of Harris, a number of authors have extended and elaborated on his insight, particularly in the case of $\alpha_p > 0$. According to Lubensky,[4] Harris and Lubensky,[5] and Grinstein and Luther,[6] quenched systems with $\alpha_p > 0$ lead to a new fixed point with $\alpha_d < 0$.

For annealed disorder Fisher[7] has shown that $\alpha_p > 0$ implies a renormalization of static exponents, so that the disordered exponent β_d is given in the terms of the pure exponent β_p via $\beta_d = \beta_p/(1-\alpha_p)$. For annealed systems with $\alpha_p < 0$, static exponents are not expected to change, though logarithmic corrections are found for $\alpha_p = 0$.

Several studies provide experimental confirmation of the theory. For Zn-doped MnF_2, a $(d,n)=(3,1)$ system with $\alpha_p > 0$, Dunlap and Gottlieb[8] found a sharp transition and a value of β_d marginally larger than β_p. They explained the smallness of the observed difference in part by a very large crossover region. For $RbMn_{0.5}Ni_{0.5}F_4$, a $(d,n)=(2,1)$ system with $\alpha_p < 0$, Birgenau, Als-Nielsen, and Shirane[9] found static exponents γ, β, and ν unchanged from pure system values. In the case of $(d,n)=(3,3)$ systems, a critical review of results for materials with small impurity concentrations ($x < 0.1\%$) provides no evidence for significant differences between β_d and β_p.[10,11]

In contrast, theory is apparently contradicted by a number of results of $(d,n)=(3,3)$ ferromagnetic alloys.[12–24] As shown in Table I, these yield values of β_d that are both substantially larger and smaller than β_p. Before accepting the results of Table I as evidence against the theory, it is important to ask if they result from disturbances not intrinsic to the phase transition. Such disturbances include: (1) the use of applied fields in all bulk measurements, (2) insufficiently close approach to T_c, (3) macroscopic alloy inhomogeneity, and (4) for hyperfine techniques, microscopic inhomogeneity of two kinds (see below). In addition, it is not clear that the theory developed for site and bond disorder applies for the amorphous systems listed in Table I.

Rather than speculate on the disturbances that may underlie the results of Table I, we present here a detailed account of recent work on *Fe*Al which we believe to be free of disturbance. The measurements and analysis reported include a model of T_c rounding, detailed comparisons to data on pure Fe, and an estimate of residual temperature and concentration gradients. The present work was preceded by a preliminary account.[14]

As will become clear, T_c rounding remains an unavoidable characteristic of our results; however, because we have ruled out other causes, we believe it

TABLE I. Experimental results for $(d,n)=(3,3)$ alloys.

Material	Method[a]	β	Ref.
Crystalline materials			
$Ni_{1-x}Cu_x$ $(0.046<x<0.188)$	bulk	0.33(1)	12
$Ni_{0.65}Rh_{0.35}$	bulk	0.476(14)	13
$Ni_{0.97}Rh_{0.03}$ ^{111}In	PAC	0.384(6)	14
$Ni_{0.983}Cu_{0.017}$ ^{111}In	PAC	0.32(2)	14
$Fe_{0.014}Pd_{0.986}$	bulk	0.464	15
$Fe_{0.96}Al_{0.04}$	ME	0.365(15)	14
Fe_xCr_{1-x} $(0.20<x<0.30)$	bulk	0.44(1) to 0.52(1)	16
Amorphous materials			
$Gd_{80}Au_{20}$	bulk	0.44(2)	17
$Ni_{36}Fe_{32}Cr_{14}P_{12}B_6$	ME	0.42(3)	18
	bulk	0.41(2)	19
$Ni_{49}Fe_{29}P_{14}B_6Si_2$	bulk	0.40(1)	20
$Fe_{80}P_{13}C_7$	bulk	0.38(2)	21
$(Fe_{1-x}Mn_x)_{75}P_{16}B_6Al_3$	bulk	0.40(3)	22
$Co_{70}B_{20}P_{10}$	bulk	0.402(7)	23
Renormalization-group theory		0.365(1)	24

[a]Method: bulk denotes macroscopic magnetization measurements using a magnetometer; PAC and ME denote local magnetization measurements using perturbed angular correlations and Mössbauer effect, respectively.

may be intrinsic to the phase transition. When our data are analyzed outside the region of rounding we find strong confirmation of the theoretical prediction that $\beta_d=\beta_p$. In fact, when analyzed with correction to scaling terms, our result $\beta_p=\beta_d=0.366(2)$ is in near perfect agreement with the RG prediction $\beta_p=0.365(1)$.[24]

We begin with a brief discussion of Mössbauer spectroscopy as applied to critical phenomena, and the reasons why *Fe*Al is likely to be a near ideal alloy choice.

II. MÖSSBAUER SPECTROSCOPY AND THE ALLOY CHOICE

Mössbauer spectroscopy, along with perturbed angular correlations and nuclear magnetic resonance, is a method which alloys determination of the local magnetization $\sigma_l(T)$ via the time-averaged hyperfine field $H(T)$. A basic assumption of the method is that near T_c $H(T)\propto\sigma_l(T)$. The correctness of this assumption has been extensively demonstrated through comparison of bulk and hyperfine critical exponents,[10,25] and through calculations based on theoretical models.[26] Hyperfine techniques provide some of the most precise static critical exponents in pure $d=3$ magnetic systems[11]; undoubtedly their greatest advantage, however, is that in contrast to bulk methods, they permit direct measurements of the spontaneous magnetization in zero applied field.

Extension of hyperfine methods from pure to disordered systems involves a number of problems that can lead to irrelevant disturbances of critical behavior, as follows.

(1) Macroscopic inhomogeneity. Generic to any method involving impurities is the possibility of macroscopic concentration gradients over the volume of the sample. Because T_c varies with impurity concentration x, such gradients may destroy the sharpness of T_c.

(2) Microscopic inhomogeneity. Even if the sample is macroscopically homogeneous it is possible that impurities will not arrange themselves randomly, but exhibit local short-range order. This can affect the hyperfine field distribution.

(3) Local environment effects. For samples that are macroscopically and microscopically homogeneous, the sum of signals received from different probe atoms will nevertheless involve several components, depending on the random variation of local environments. This can happen in two ways: (a) quadrupole interactions from different neighbor configurations of impurity atoms will produce a combined electric-magnetic interaction at the probe nucleus and (b) impurity atoms that produce disturbances of host moments will cause a distribution of

magnetic interactions.

Because these effects are not easily corrected once data are recorded, it is best to avoid them through judicious choice of sample composition. Effects of concentration inhomogeneity can be minimized by choosing an alloy for which dT_c/dx is small. Microscopic short-range order is best avoided by quenching the sample from high temperature. Local moment disturbances are eliminated by choosing an alloy for which impurities have little effect on neighboring host atoms. Effects of quadrupole interaction are reduced by choosing probe atoms for which the quadrupole interaction frequency due to neighboring charge defects is a small fraction of the magnetic interaction frequency.

In earlier work[14] we compared measurements on three dilute magnetic alloys (*Fe*Al, *Ni*Rh, and *Ni*Cu) and concluded both on experimental and theoretical grounds that *Fe*Al best avoids irrelevant local environment disturbances near T_c (see Table II). Independently, we have made a comparison of local environment parameters in 50 Fe and Ni alloys,[27] and this leads to the conclusion that *Fe*Al is the single best choice among the 50. We are thus reasonably confident that we cannot choose a significantly better alloy for studying the effect of disorder on critical behavior.

III. PRELIMINARY RESULTS

Initially[14] we studied $H(T)$ using the ^{57}Fe Mössbauer effect in an $Fe_{0.96}Al_{0.04}$ absorber. The sample had been produced by melting, rolling, and annealing at 1100 K, and quenching to room temperature, and was provided by F. van der Woude of the University of Groningen. Similar samples had been previously characterized by Maring[28] in detailed studies of hyperfine field shifts. Our measurements were made in the range $295 \leq T \leq 1050$ K with a constant acceleration spectrometer of standard design, a 10 mCi ^{57}Co*Pd* source, and a two-stage oven[29] having a long-term stability of 0.05 K.

Typical data, shown in Fig. 1, exhibit well-defined satellites due to randomly placed Al atoms.[28] We fit these with a superposition of two six-line spectra having a relative spacing as required by the nuclear Zeeman effect. We found that the linewidth remains constant at 0.27 mm/s (full width at half maximum) to reduced temperatures $t \equiv (1-T/T_c) \simeq 1.5\times10^{-3}$. Checks of the linewidth above T_c, as well as splitting below T_c, show that the electric quadrupole interaction is less than 0.03 mm/s, as expected.

As in previous Mössbauer work on pure Fe (Refs. 30 and 31) we identified T_c via a relatively sharp break in the centroid velocity transmission (CVT), and independently, from the T intercept of the linearized hyperfine field $H(T)^{1/0.38}$. The value found for T_c is about 4 K lower than in pure Fe, as expected from the fact that $dT_c/dx = -0.90$ K/at. % Al (see Table II).

Spectra for reduced temperatures $t \leq 10^{-3}$ showed unresolved structure. To obtain $H(T)$ in this region, the data were fitted by assuming a linewidth of 0.27 mm/s, as observed in the well-resolved region. This leads to anomalously high values of the linearized field. Because of the favorable characteristics of *Fe*Al with respect to local environment disturbances, and the belief that quenching had removed any macroscopic inhomogeneity in Al concentration, this behavior was attributed to possible residual temperature gradients.

To analyze critical behavior the data from the unresolved region were excluded, and the remainder was fitted with

TABLE II. Suitability of three alloys for hyperfine experiments.

Alloy	Probe	ω_0[a] (Mrad/s)	ω_L[b] (Mrad/s)	ω_0/ω_L	dT_c/dx[c] (K/at. %)	$\Delta\mu/\mu_h$[d] (%)	$(1-T/T_c)_{min}$[e]
*Ni*Cu	^{111}Cd	89	98	0.9	−11	−6	2×10^{-2}
*Ni*Rh	^{111}Cd	89	98	0.9	−11	0	10^{-2}
*Fe*Al	^{57}Fe	15	250	0.06	−0.9	0	2×10^{-3}

[a] ω_0 is the quadrupole interaction frequency for a nearest-neighbor point charge.
[b] ω_L is the Larmor frequency at 300 K in the pure host.
[c] dT_c/dx is the concentration dependence of T_c [see S. J. M. Stoelinga *et al.*, J. Phys. 32, (Paris) Colloq. C1-330 (1971)].
[d] $\Delta\mu/\mu_h$ is the moment disturbance on host atoms neighboring an impurity atom [see G. G. Low, Adv. Phys. 18, 371 (1969)].
[e] $(1-T/T_c)_{min}$ is the smallest reduced temperature for which unambiguous measurements of $H(T)$ could be made [see A. Chowdhury *et al.*, Hyperfine Interact. 10, 893 (1981)].

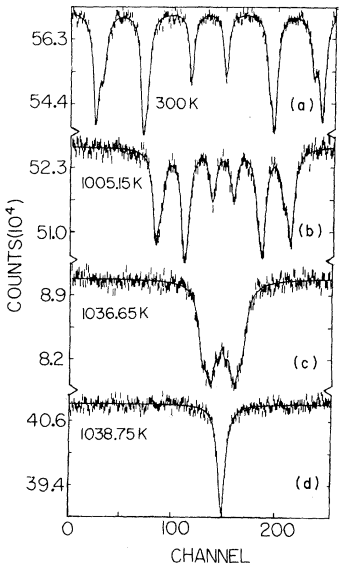

FIG. 1. Sample ^{57}Fe Mössbauer spectra for $Fe_{0.96}Al_{0.04}$ at temperatures below and above T_c. Below T_c (spectra *a*, *b*, and *c*), the data are fit to two six-line patterns. The high-field spectra corresponds to Fe without Al in the nearest-neighbor shell; the low-field spectra correspond to Fe with one Al nearest neighbor.

$$h(T)=B(1-T/T_c)^{\beta} \tag{1}$$

with B, T_c, and β as free parameters. Here $h(T)=H(T)/H(0)$ is the reduced hyperfine field. Equation (1) describes the leading singular term in the magnetization near T_c, and is expected to be asymptotically correct. To find the value of β we conducted a range-of-fit analysis[10,11] in which the most distant point from T_c is successively excluded from the fit to Eq. (1). This leads to effective values of β which converge to the asymptotic value. Our conclusion was that $\beta=0.365(15)$, a result that compares favorably with experiments on pure Fe (Refs. 30 and 31) and with the predictions of RG theory for the isotropic Heisenberg model.[24]

Thus, except for the anomalous behavior in the unresolved region, our results confirm the predictions of theory for systems with $\alpha_p<0$: i.e., disorder has no effect on static critical phenomena.

IV. UNDERSTANDING THE ANOMALOUS BEHAVIOR NEAR T_c

It was the goal of recent work on *Fe*Al to understand in detail the anomalous behavior near T_c. We approached this problem in five ways as follows.

(1) To control possible T_c rounding due to thermal gradients we made direct measurements of temperature differences.

(2) To check for possible macroscopic inhomogeneity we studied our samples via electron microprobe analysis.

(3) To observe possible effects of improvements in thermal uniformity and to study the effects of Al concentration, we did new measurements on $Fe_{0.96}Al_{0.04}$ and $Fe_{0.99}Al_{0.01}$.

(4) To characterize the measurements in a more general way than before, we fitted data near T_c with a single-line paramagnetic component as well as two six-line ferromagnetic components.

(5) To describe the structure of the anomalous behaviour near T_c, we interpreted the new data and previous data on Fe and $Fe_{0.96}Al_{0.04}$ via a simple model of T_c rounding.

Thermal gradient measurements. Thermal gradients affecting the measurements were estimated by embedding thermocouple junctions at the center and at the outside edge of the 8-mm diameter BeO disks clamping the absorber foil. With the use of a differential measurement technique, it was found that the temperature gradient over the 4-mm radius of the foil was no more than 0.1 K. Given the cylindrical geometry of the oven,[29] this must be regarded as an upper limit. The result is consistent with earlier measurements on Mössbauer sources.[30] Since the value 0.1 K is much smaller than the range of the anomalous region for the alloys ($\sim$2 K), thermal gradients must be ruled out as a significant cause of T_c rounding.

Electron microprobe analysis. Both $Fe_{0.96}Al_{0.04}$ and $Fe_{0.99}Al_{0.01}$ foils were scanned with a 60-keV, 1-μm-diameter electron beam, using energy dispersive x-ray detection. As shown in Table III, by using the intensity of Al K x rays (sensitive to a depth of 5000 Å), we found substantial surface segregation of Al. This is an effect that is apparently well known for *Fe*Al.[32] At the same time, transverse scans made on a cut in the nominally 4 at. % Al foil showed that the bulk Al concentration was constant to within the statistical error of the measurement. Given the absolute accuracy of the microprobe technique ($\pm$0.5 at. %) the average value of 4.6 at. % Al is consistent with the nominal Al concentration obtained from weighing prior to making the alloy.

Since $dT_c/dx=-0.9$ K/at. % for Al in Fe, the results suggest an upper limit on T_c smearing of $\Delta T_c=0.4$ K, a value too small to explain the extent of the observed rounding.

Electron microprobe analysis, of course, does not

TABLE III. Results of electron microprobe analysis. (Measurements were made under contract by Photometrics, Woburn, MA.)

	$Fe_{0.96}Al_{0.04}$	$Fe_{0.99}Al_{0.01}$
Sample		
Nominal Al concentration (at. %)	4	1
Surface scan		
Number of measurements	17	3
Average concentration with standard deviation (at. %)	22(6)	2.2(4)
Transverse scan		
Number of measurements	15	
Average concentration with standard deviation (at. %)	4.6(2)	

rule out Al segregation on a scale smaller than 1 μm. On this point, however, there is a rather convincing argument based on the character of the Mössbauer spectra. It begins with the fact that Maring was able to fit his spectra with a model that assumes random distribution of Al atoms.[28] Combined with the fact that we observed no change in the satellite structure after $\sim$30 days near T_c, one concludes that the Al atoms have not moved from their random configuration.

New data. To assess improvements made in the sample geometry and to study the effect of variation in the Al concentration, we made new measurements on alloys with the nominal composition $Fe_{0.96}Al_{0.04}$ and $Fe_{0.99}Al_{0.01}$. The new data for $Fe_{0.96}Al_{0.04}$ are distinguished by a particularly wide temperature range, covering $1.3\times10^{-3}\leq t\leq0.392$. The new data also involved special precautions to reduce temperature gradients below the values encountered in previously published results.

Extended data analysis. Our main concern in renewed data analysis was the region near T_c in which spectra are unresolved. In fitting this region the paramagnetic linewidth, intensity ratios, and relative line positions were fixed to values observed in the well-resolved region far from T_c. As before[14] the characteristics of ferromagnetic spectra corresponded closely to the behavior observed by Maring.[28] In addition, a well-defined paramagnetic fraction was found as far as 2 K below T_c. The ratio of fields for one and zero Al neighbors was 92%, independent of temperature. Therefore only values of $H(T)$ for isolated probes are quoted below.

Fitted parameters of interest, in addition to $H(T)$, include the linewidth of ferromagnetic spectra, the paramagnetic fraction, and the centroid velocity transmission (CVT). The linewidth analysis involves some error since the strong overlap of absorption lines makes our sum of Lorentzian formulation only approximately correct. Nevertheless, we believe it provides a useful qualitative comparison between the alloy and pure Fe measurements.

Our analysis was uniformly applied to all previous data on pure Fe,[30,31] previous alloy data,[14] as well as the present data. Results for Fe absorber measurements and new data on *Fe*Al are compared in Figs. 2–4. This leads to the following conclusions.

(1) For the pure Fe absorber (Fig. 2) the linearized hyperfine field intercept and the CVT break show no significant difference; a paramagnetic

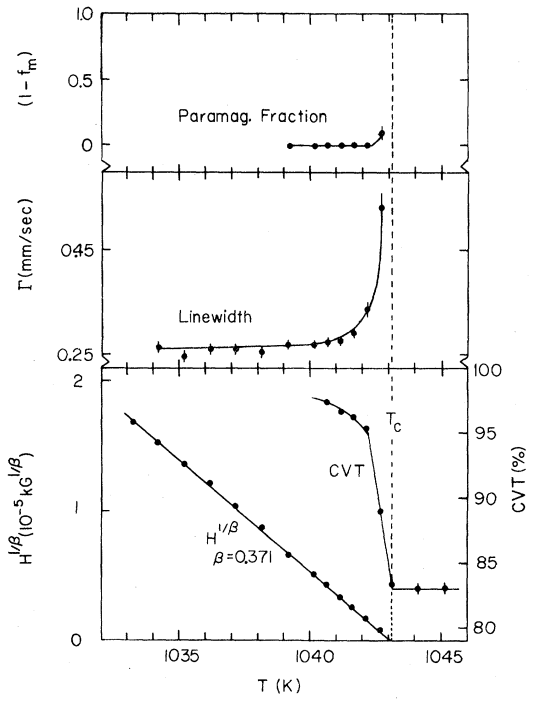

FIG. 2. Paramagnetic fraction, linewidth, linearized hyperfine field, and centroid velocity transmission for Fe. The paramagnetic fraction is small; the line broadening is explained by the overlap of Lorentzian components, and there is no apparent difference between the linearized hyperfine field and the break in the CVT. Taken together, these indicators provide little evidence for T_c rounding.

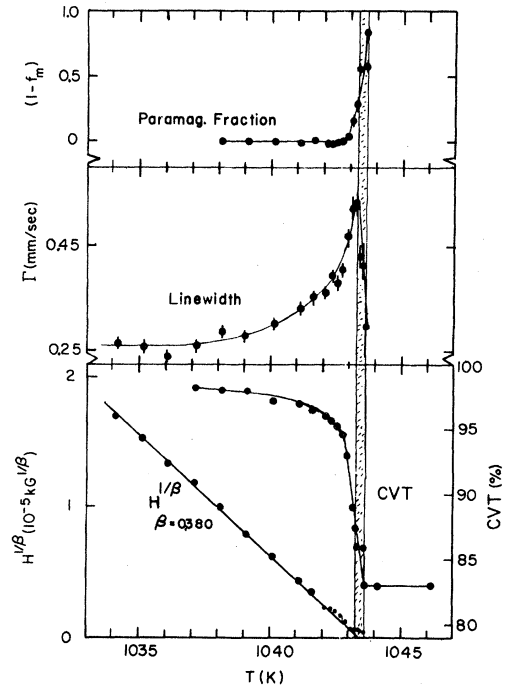

FIG. 3. Paramagnetic fraction, linewidth, linearized hyperfine field, and centroid velocity transmission for $Fe_{0.99}Al_{0.01}$. Compared to pure Fe the paramagnetic fraction is significant; the linewidth shows broadening beyond the amount explained by overlapping lines; the linearized hyperfine field near T_c lies above the extrapolation from low temperature; and there is a detectable difference between the extrapolated linearized field and the CVT break. Taken together, these effects are interpreted in terms of a T_c spread of 0.3 K (shaded band).

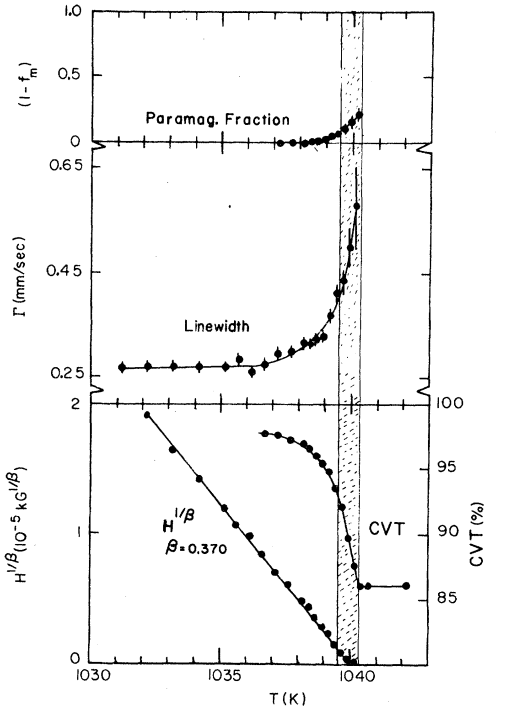

FIG. 4. Paramagnetic fraction, linewidth, linearized hyperfine field, and centroid velocity transmission for $Fe_{0.96}Al_{0.04}$. The observed effects are comparable to, though larger than, those seen for $Fe_{0.99}Al_{0.01}$ in Fig. 3, and are interpreted in terms of a T_c spread of 0.8 K (shaded band).

component is barely detectable; the linewidth shows little broadening except within a degree of T_c; and the hyperfine field has no anomaly near T_c. Results found for the Fe source measurement are similar, except that the linewidth shows no broadening.

(2) For the alloy samples (Figs. 3 and 4) the temperature at which the CVT breaks is significantly different from the T intercept of the extrapolated linearized hyperfine field; a significant paramagnetic component appears within 2 K of T_c; the linewidth shows greater broadening extending as far as 5 K below T_c; and the hyperfine field exhibits noticable anomalies near the T intercept.

A model for rounding. To understand the effects indicated in Figs. 2–4 we assume different portions of the sample have different Curie temperatures. For a given temperature T this implies a distribution of hyperfine fields, $H(T,T_c)p(T_c)dT_c$, where $p(T_c)dT_c$ is the fraction of the sample having Curie temperature in the range T_c to T_c+dT_c. To make useful calculations with this model we assume that the hyperfine field has the usual singular form

$$H(T,T_c)=\begin{cases}B(1-T/T_c)^{\beta}, & T<T_c \quad (2a)\\ 0, & T>T_c\ . \quad (2b)\end{cases}$$

With specification of the factor $p(T_c)$ it is then possible to calculate the paramagnetic fraction, the mean field, the linewidth, and the centroid velocity transmission as described in the Appendix. With T_c constrained to the interval $T_1 \le T_c \le T_2$ one finds for temperatures $T > T_1$ (1) substantial deviation of the mean linearized field from a straight line, (2) a significant paramagnetic fraction, and (3) a linewidth anomaly. In addition there is a distinct difference between the break in the CVT and the T intercept of the linearized hyperfine field extrapolated from low temperature. Together these features reproduce all essential aspects of the data.

We therefore apply the model to interpret the data as follows. The upper limit of the T_c distribution T_2 is taken as the break in the CVT. The T intercept obtained by extrapolating the linearized hyperfine field from the spectrally resolved region is taken as the mean Curie temperature $\bar{T}_c$. The width of the Curie temperature distribution is taken as $\Delta T_c = 2(T_2 - \bar{T}_c)$. Values of T_2, $\bar{T}_c$, and ΔT_c for each of five sets of data are listed in Table IV. From this we see that, within statistics, $\Delta T_c = 0$ for pure Fe, whereas $\Delta T_c \simeq 0.3$ K and $\Delta T_c = 1.0$ K for the 1 at. % and 4 at. % Al samples, respectively. In addition we find for the two measurements on $Fe_{0.96}Al_{0.04}$ there is only a marginally small difference in ΔT_c, even though in one set of measurements (labeled by footnote e) thermal gradients are known to contribute a smearing $\Delta T_c \leq 0.1$ K.

We conclude, therefore, that the anomalous behavior near the phase transition may be explained by a T_c distribution whose width is directly linked to the Al concentration. Since concentration gradients of the requisite size have not been found through microprobe analysis, and examination of satellite structure in the Mössbauer spectra suggest a random placement of the Al atoms, it is possible that the observed effects are fundamental aspects of the phase transition.

V. CRITICAL EXPONENT VALUES

For the purpose of extracting critical exponents β we have analyzed or reanalyzed all Mössbauer measurements on Fe and *Fe*Al obtained to data in our laboratory. These include source and absorber measurements on pure Fe by Kobeissi,[30,31] our previously published work on $Fe_{0.96}Al_{0.04}$ and the measurements on $Fe_{0.96}Al_{0.04}$ and $Fe_{0.99}Al_{0.01}$ discussed here for the first time. Because none of the hyperfine field values have been previously listed, we give $H(T)$ vs T for all five data sets in Table V.

Guided by our study of T_c rounding, we excluded absorber measurements for which (1) the CVT plot had fallen by one-third of its total drop, (2) there was any evidence of a paramagnetic component, or (3) the value of T was within $1.5\Delta T_c$ of $\bar{T}_c$. The first criterion avoids problems related to the sum-of-Lorentzian approximation used in fitting the Mössbauer spectra. The second and third criteria reduce problems related to the distribution of T_c. The source measurement on Fe was affected only by the second criterion. For reference, $t_{\min}$, the minimum reduced temperature included in each analysis, is indicated in Table IV. Data points excluded on account of these criteria are so indicated in Table V.

Range-of-fit analysis. As a first approach to extracting the critical exponent β we fitted the reduced hyperfine field to Eq. (1) over varying temperature intervals, as already described in Sec. III. Plots of the effective value of β as a function of the maximum included reduced temperature are shown in Fig. 5. From this effective asymptotic values of β, B, and T_c were deduced, as listed in Table VI.

It can be seen from Table VI that all five data sets yield asymptotic values of β in the range of $0.365 \leq \beta \leq 0.380$. Computer modeling of the rounding in the alloy samples suggests that "asymptotic" exponents deduced by range-of-fit analysis should be corrected upward by about 0.01. Applying this correction to the 4 at. % alloy samples brings all deduced exponents into the range $0.371 \leq \beta \leq 0.380$.

We conclude that except for the residual rounding, there is no significant difference between pure and disordered samples. If we take $\beta = 0.375(5)$ as

TABLE IV. Summary of results on T_c distribution.

Description at. % Al	T_2 (K)	$\bar{T}_c$ (K)	ΔT_c (K)	$t_{\min}$	Data source
0 source	1042.85(5)	1042.91(4)	−0.1(1)	12×10^{-4}	a
0 absorber	1042.9(2)	1043.10(8)	−0.4(4)	7×10^{-4}	b
1 absorber	1043.60(5)	1043.45(10)	0.3(1)	7×10^{-4}	c
4 absorber	1038.25(10)	1037.7(2)	1.1(4)	15×10^{-4}	d
4 absorber	1040.3(1)	1039.9(1)	0.8(3)	22×10^{-4}	e

[a]M. A. Kobeissi and C. Hohenemser, Ref. 30.
[b]M. A. Kobeissi, Phys. Rev. B 24, 2380 (1981).
[c]This work.
[d]A. R. Chowdhury, C. Allard, R. M. Suter, G. S. Collins, C. Hohenemser, and M. A. Kobeissi, Hyperfine Interact. 10, 893 (1981).
[e]This work.

TABLE V. Hyperfine field versus temperature.

T (K)	H (kG)	T (K)	H (kG)	T (K)	H (kG)	T (K)	H (kG)
	^{57}Co*Fe* source[a]				$Fe_{0.99}Al_{0.01}$ absorber[c]		
1042.78[f]	24.8(47)	1042.65[f]	28.2(49)	1034.15	96.9(2)	1033.15	101.6(2)
1042.28[f]	30.1(22)	1041.65	44.0(14)	1031.15	108.6(2)	1029.15	113.8(1)
1041.14	50.3(7)	1040.15	58.9(7)	1027.15	118.4(2)	1025.15	122.3(1)
1039.15	65.4(4)	1038.15	73.2(4)	1020.15	132.9(2)	1005.15	157.5(1)
1037.15	78.6(4)	1036.15	83.7(4)				
1035.15	87.2(4)	1034.15	91.4(4)		$Fe_{0.96}Al_{0.04}$ absorber[d]		
1032.15	99.6(4)	1031.15	102.8(4)	1038.15[f]	8.5(66)	1037.90[f]	22.3(38)
1030.15	106.1(4)	1029.15	108.7(4)	1037.40[f]	25.3(36)	1037.0[f]	33.9(10)
1026.15	117.6(4)	1024.15	122.3(4)	1036.65[f]	42.2(3)	1036.15	47.8(10)
1020.27	129.9(4)	1016.73	136.6(8)	1035.15	56.4(5)	1034.15	65.3(6)
1010.15	148.1(4)	1000.02	162.7(4)	1033.15	70.9(4)	1032.15	77.7(3)
994.40	166.2(4)	986.90	175.4(4)	1031.15	82.7(5)	1030.15	86.9(3)
947.77	205.3(4)	867.52	241.5(4)	1029.15	90.6(5)	1028.15	94.4(3)
820.77	256.7(4)	684.90	285.6(4)	1027.15	97.8(3)	1026.15	102.3(3)
				1024.15	107.8(3)	1022.15	122.2(3)
	Fe absorber[b]			1020.15	117.2(3)	1015.15	128.7(3)
1042.70[f]	30.9(15)	1042.40	36.0(5)	1010.15	137.0(4)	1005.15	145.5(2)
1042.15	39.6(2)	1041.65	47.7(2)				
1041.15	51.8(2)	1040.65	57.3(2)		$Fe_{0.96}Al_{0.04}$ absorber[e]		
1040.15	61.5(3)	1039.15	67.9(2)	1040.15[f]	13.7(30)	1039.90[f]	21.6(15)
1038.15	75.5(2)	1037.15	80.3(2)	1039.65[f]	29.1(6)	1039.40[f]	35.0(4)
1036.15	85.4(2)	1035.15	89.0(2)	1039.15[f]	41.9(7)	1038.90[f]	44.8(5)
1034.15	92.9(2)	1033.15	96.5(2)	1038.65[f]	48.7(4)	1038.40[f]	52.3(2)
1032.15	100.8(2)	1031.15	103.9(2)	1038.15[f]	54.3(3)	1037.65	59.2(3)
1030.15	106.9(2)	1029.15	109.3(2)	1037.15	62.4(3)	1036.65	66.5(3)
1026.15	117.3(2)	1024.15	122.1(2)	1036.15	70.5(5)	1035.65	72.4(3)
1020.15	130.2(2)	1015.15	139.6(2)	1035.15	75.3(3)	1034.15	80.7(2)
1010.15	147.5(2)			1033.15	84.9(3)	1032.15	89.5(2)
				1031.15	93.6(2)	1030.15	96.9(2)
	$Fe_{0.99}Al_{0.01}$ absorber[c]			1029.15	100.3(2)	1028.15	103.6(2)
1043.65[f]	26.0(20)	1043.53[f]	27.2(25)	1026.65	109.1(2)	1025.15	112.4(2)
1043.40[f]	29.0(33)	1043.28[f]	28.2(15)	1023.15	118.4(2)	1021.15	123.4(2)
1043.15[f]	28.7(10)	1042.95[f]	35.2(3)	1018.65	128.6(2)	1016.15	133.8(2)
1042.75	39.5(3)	1042.55	42.5(5)	1010.15	143.9(2)	1003.15	155.0(2)
1042.35	45.2(5)	1042.15	48.2(3)	990.15	169.7(1)	977.15	182.5(2)
1041.65	53.6(3)	1041.15	59.0(3)	967.15	190.1(2)	956.15	198.4(2)
1040.15	66.1(2)	1039.15	72.6(2)	944.15	206.3(2)	931.15	214.6(2)
1038.15	79.5(2)	1037.15	84.6(2)	834.15	253.7(2)	728.15	279.0(3)
1036.15	88.4(2)	1035.15	92.9(2)	631.03	294.9(2)		

[a]M. A. Kobeissi and C. Hohenemser, Ref. 30.
[b]M. A. Kobeissi, Phys. Rev. B 24, 2380 (1981).
[c]This work.
[d]A. R. Chowdhury, C. Allard, R. M. Suter, G. S. Collins, C. Hohenemser, and M. A. Kobeissi, Hyperfine Interact. 10, 893 (1981).
[e]This work.
[f]Data points excluded from critical exponent determinations (see text).

the ensemble mean for the five data sets, it appears that the experimental value is somewhat higher than the RG prediction of $\beta=0.365(1)$.

Correction-to-scaling analysis. A possible explanation for the remaining apparent discrepancy between theory and experiment is that any analysis based on Eq. (1) involves errors due to the neglect of correction-to-scaling terms. To investigate this pos-

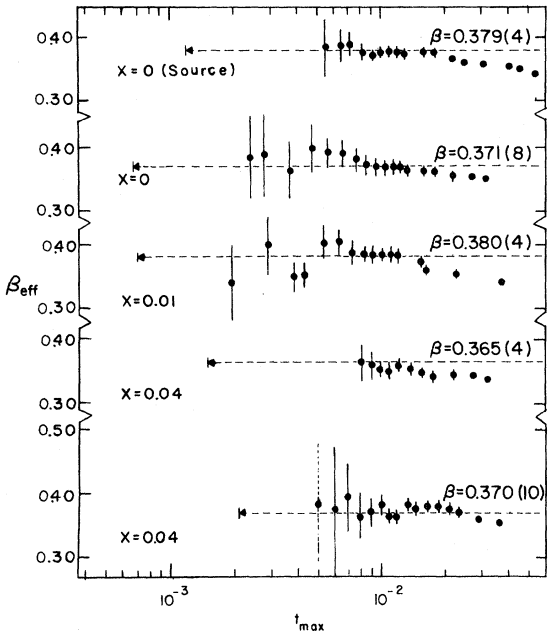

FIG. 5. Range-of-fit analysis for the five data sets. The data, from top to bottom, correspond to the Fe source, the Fe absorber, $Fe_{0.99}Al_{0.01}$, and two cases of $Fe_{0.96}Al_{0.04}$, respectively. Arrowheads indicate the lower limit, and t_{max} the maximum value of reduced temperature included in each fit. Dashed lines represent the asymptotic value of β read from the plot.

sibility we have fitted the data with

$$h(t)=Bt^{\beta}(1+a_m t^{\Delta}+a_n x t^{|\alpha|}) . \quad (3)$$

Here x is the Al concentration, a_m and a_n are amplitudes, and Δ and α are exponents predicted via RG theory.[24] The first term is the leading singular term near T_c, and corresponds to Eq. (1), the second term describes corrections to scaling at finite t, and the third represents the effect of impurities on critical behavior.[33] In all fits to Eq. (3) the exponents Δ and α were fixed to their RG values (i.e., $\Delta=0.55$, $\alpha=-0.125$) and T_c was treated as a free parameter. The analysis was carried out in three steps as follows.

1. Fits with $a_n=0$. Since x is zero or small for all five cases, the contribution of $a_n x t^{|\alpha|}$ is likely to be small. As a first approximation we therefore set $a_n=0$, and attempt to fit with β, B, a_m, and T_c free. As shown in Table VII top, this process yields well-defined results when the reduced temperature ranges to $t=0.4$, but fails to converge for data covering a smaller range of t. There is no significant difference between exponents and amplitudes found for pure Fe and $Fe_{0.96}Al_{0.04}$; and the values obtained for β are significantly lower than before. The first finding supports the correctness of the assumption $a_n=0$. The second finding indicates that the range-of-fit analysis is probably affected by neglect of the term $a_m t^{\Delta}$.

2. Fits with β and B fixed. To demonstrate in another way that the product $a_n x$ is near zero, we fixed β and B at the values found above for pure Fe, and fitted all data sets with a_m, a_n, and T_c free. The results are summarized in Table VII, middle.

3. Fits with $a_n=0$, B, and a_m fixed. To obtain fitted values for the three data sets that were nonconvergent in step 1, we took $a_n=0$ as in step 1, and in addition fixed B and a_m to the values obtained for $Fe_{0.96}Al_{0.04}$ in step 1, while leaving only β and T_c free. The results shown in Table VII, bottom, indicate that all values of β are now consistent.

Fitting the data with an equation that includes correction to scaling terms therefore appears to be more satisfactory on several grounds. (1) For data covering a large range of t, the approach provides more precisely defined values of B and β than

TABLE VI. Summary of range-of-fit analysis.

Description at. % Al	β	B	T_c (K)	Data source
0 source	0.379(4)	1.66(3)	1042.91(4)	a
0 absorber	0.371(8)	1.62(5)	1043.05(8)	b
1 absorber	0.380(4)	1.71(4)	1043.61(5)	c
4 absorber	0.365(4)	1.50(4)	1037.44(7)	d
4 absorber	0.370(10)	1.64(3)	1040.38(10)	e

[a]M. A. Kobeissi and C. Hohenemser, Ref. 30.
[b]M. A. Kobeissi, Phys. Rev. B 24, 2380 (1981).
[c]This work.
[d]A. R. Chowdhury, C. Allard, R. M. Suter, G. S. Collins, C. Hohenemser, and M. A. Kobeissi, Hyperfine Interact. 10, 893 (1981).
[e]This work.

TABLE VII. Summary of correction-to-scaling analysis.

Fixed parameters: $\Delta=0.55$, $\alpha=-0.125$, $a_n=0$

Description at. % Al	t_{max}	Fitted parameters β	B	a_m	T_c	Data source
0 source	0.342	0.368(5)	1.67(3)	−0.46(2)	1042.42(13)	a
0 absorber	0.035		Fitting did not converge			b
1 absorber	0.036		Fitting did not converge			c
4 absorber	0.031		Fitting did not converge			d
4 absorber	0.392	0.365(3)	1.66(2)	−0.44(2)	1039.81(12)	e

Fixed parameters: $\Delta=0.55$, $\alpha=-0.125$, $\beta=0.368$, $B=1.67$

Description at. % Al	t_{max}	Fitted parameters a_m	$a_n x$	T_c	Data source
0 source	0.342	−0.46(2)	0	1042.42(13)	a
0 absorber	0.035	−0.50(2)	0	1042.87(8)	b
1 absorber	0.036	−0.43(7)	0.01(2)	1043.42(6)	c
4 absorber	0.031	−0.43(20)	−0.02(5)	1037.44(23)	d
4 absorber	0.392	−0.45(1)	0.00(3)	1039.81(6)	e

Fixed parameters: $\Delta=0.55$, $\alpha=-0.125$, $B=1.66$, $a_m=-0.44$, $a_n=0$.

Description at. % Al	t_{max}	Fitted parameters β	T_c	Data source
0 source	0.342	0.366(1)	1042.46(9)	a
0 absorber	0.035	0.368(1)	1042.91(3)	b
1 absorber	0.036	0.363(1)	1043.33(5)	c
4 absorber	0.031	0.369(1)	1037.52(16)	d
4 absorber	0.392	0.365(3)	1039.81(12)	e

[a]M. A. Kobeissi and C. Hohenemser, Ref. 30.
[b]M. A. Kobeissi, Phys. Rev. B 24, 2380 (1981).
[c]This work.
[d]A. R. Chowdhury, C. Allard, R. M. Suter, G. S. Collins, C. Hohenemser, and M. A. Kobeissi, Hyperfine Interact. 10, 893 (1981).
[e]This work.

range-of-fit-analysis, and gives a consistent value for the amplitude a_m. (2) As before, deduced values of β show no significant dependence on Al concentration, but in comparison to range-of-fit analyses they are consistently lower with an average of $\beta=0.366(2)$. This is in more or less perfect agreement with RG theory. (3) Varying Al concentration appears to have an undetectably small effect on the correction-to-scaling amplitudes a_m and a_n, and suggests that a_n is of order unity or smaller.

VI. SUMMARY

In this paper we studied the zero-field magnetization of a disordered $d=3$ Heisenberg ferromagnet using hyperfine fields measured via the Mössbauer effect. Our principal findings are as follows.

(1) Mössbauer measurements on dilute *Fe*Al avoid irrelevant disturbances due to signal complexity and sample inhomogeneity through the special properties of the alloy. Moreover, the system appears closely related to the site disorder models studied by theorists.

(2) Even with such an advantageous system, there is evidence for a T_c distribution ~ 1 K in width. A model was developed to help interpret the observed rounding behavior, and to assess possible bias of fitting. Only a fraction of the observed rounding can be explained by residual thermal gradients or concentration nonuniformity on a scale of 1 μm or larger.

(3) Outside the region of rounding systematic range-of-fit analyses to determine β for pure Fe and *Fe*Al yielded equivalent values, with an average corrected value of $\beta=0.375(5)$. This is in fair

agreement with the renormalization-group prediction of $\beta=0.365(1)$.

(4) Outside the region of rounding, analysis of correction-to-scaling terms yielded consistent results for the first correction-to-scaling amplitude, provided Δ is fixed at its RG value. In addition, the analysis again produced equivalent values of β for Fe and *Fe*Al. The average over the five data sets is now $\beta=0.366(2)$, in more or less perfect agreement with RG predictions.

Except for the in part unexplained rounding of T_c, these results conclude our search for the effects of Al impurities on the static critical behavior of Fe in a resounding null result. If *Fe*Al is representative of disordered Heisenberg ferromagnets, the wide scatter in previous results (Table I) is likely to be caused by unrecognized systematic errors. We have already stated in the Introduction to this paper what we think these errors might be.

ACKNOWLEDGMENTS

We are indebted to F. van der Woude of the University of Groningen for providing the alloy samples. We thank M. A. Kobeissi for experimental assistance in the early stages of this work, and for the design of the Mössbauer oven. We thank A. Aharony for suggesting the use of Eq. (3) in the critical exponent analysis, and acknowledge helpful discussions with J. I. Budnick and G. Mazenko. This work was supported by the National Science Foundation through Grants Nos. DMR 77-01250 and DMR 80-02443.

APPENDIX: A MODEL FOR ROUNDING

As discussed in the text, it is assumed that different portions of the sample have different Curie temperatures. Hence we consider a distribution of hyperfine fields, $H(T,T_c)p(T_c)dT_c$, where $p(T_c)dT_c$ is the fraction of the sample having a Curie temperature in the interval (T_c,T_c+dT_c). We assume, further, that each field component takes the form

$$H(T,T_c)=\begin{cases}B(1-T/T_c)^{\beta}, & T\le T_c \quad \text{(A1)}\\ 0, & T\ge T_c \quad \text{(A2)}\end{cases}$$

in which B is assumed independent of T_c. With these assumptions, quantities of interest to our experiments may be expressed as follows. The fraction of the sample that is ferromagnetic is

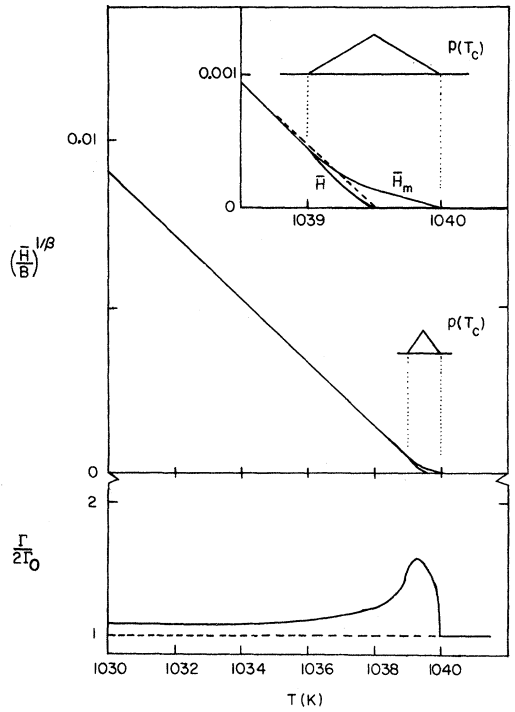

FIG. 6. Computed linearized hyperfine field (top) and linewidth anomaly (bottom) as obtained from the model of T_c rounding explained in the text. The assumed distribution of Curie temperatures, $p(T_c)$, is shown in the inset.

$$f_m(T)=\int_T^{\infty} p(T_c)dT_c \ . \quad \text{(A3)}$$

The average hyperfine field (including a possible paramagnetic component) is

$$\bar{H}(T)=\int_T^{\infty} H(T,T_c)p(T_c)dT_c \ . \quad \text{(A4)}$$

The average hyperfine field of the ferromagnetic portion of the sample (actually measured) is

$$\bar{H}_m(T)=\int_T^{\infty} H(T,T_c)p(T_c)dT_c \Big/ \int_T^{\infty} p(T_c)dT_c \ , \quad \text{(A5)}$$

and the linewidth arising from the field distribution in the ferromagnetic portion is proportional to

$$\Delta H_m(T)=(\overline{H_m^2}-\bar{H}_m^2)^{1/2} \ . \quad \text{(A6)}$$

The quantities $\bar{H}_m$ and ΔH_m may be expressed in terms of $\bar{H}$ and f_m by

$$\bar{H}_m(T)=\bar{H}(T)/f_m \ , \quad \text{(A7)}$$

$$\Delta H_m(T)=(\overline{H^2}/f_m-\bar{H}^2/f_m^2)^{1/2} \ . \quad \text{(A8)}$$

With these relations it is possible to compute all desired quantities by evaluating just f_m and $\bar{H}$.

To illustrate the model we assume $p(T_c)$ is triangular, ranging from $T_1 = 1039$ K to $T_2 = 1040$ K, and that $\beta = 0.38$. The results of our calculations, illustrated in Fig. 6, indicate the following.

(1) In the region $T_1 \leq T \leq T_2$ the linearized hyperfine field $\bar{H}_m^{1/0.38}$ lies significantly above the line extrapolated from low temperature.

(2) There is a linewidth anomaly which extends significantly beyond the interval $T_1 < T < T_2$.

(3) Extrapolation of $\bar{H}^{1/0.38}$ from low temperature leads to the mean value of the Curie temperature $\bar{T}_c$ that lies halfway between T_1 and T_2 when $p(T_c)$ is symmetric.

(4) For temperatures $1.5(T_2 - T_1)$ below $\bar{T}_c$ there is little difference between the actual value of the linearized hyperfine field and the line extrapolated from low temperature. It appears, therefore, that a reliable value of β will be obtained if data down to $1.5(T_2 - T_1)$ below $\bar{T}_c$ are excluded.

Although these results are by no means general, because they reproduce our experimental results in sufficient detail, we believe they may be used to define the region for which critical behavior is essentially "undisturbed" by rounding.

[1]B. M. McCoy and T. T. Wu, Phys. Rev. Lett. 23, 383 (1968); Phys. Rev. 176, 631 (1968).

[2]H. Au-Yang, M. E. Fisher, and A. E. Ferdinand, Phys. Rev. B 13, 1238 (1976); H. Au-Yang, *ibid.* 13, 1266 (1976).

[3]A. B. Harris, J. Phys. C 7, 1671 (1974).

[4]T. C. Lubensky, Phys. Rev. B 11, 3573 (1975).

[5]A. B. Harris and T. C. Lubensky, Phys. Rev. Lett. 33, 1540 (1974).

[6]G. Grinstein and A. Luther, Phys. Rev. B 13, 1329 (1976).

[7]M. E. Fisher, Phys. Rev. 176, 257 (1968).

[8]R. A. Dunlap and A. M. Gottlieb, Phys. Rev. B 23, 6106 (1981).

[9]R. Birgeneau, J. Als-Nielsen, and G. Shirane, Phys. Rev. B 16, 280 (1977).

[10]C. Hohenemser, T. A. Kachnowski, and T. K. Bergstresser, Phys. Rev. B 13, 3154 (1976).

[11]R. M. Suter and C. Hohenemser, J. Appl. Phys. 50, 1814 (1979).

[12]E. E. Anderson, S. Arajs, A. A. Stelmach, B. L. Tehan, and Y. D. Yao, Phys. Lett. 36, 173 (1971).

[13]W. C. Muellner and J. S. Kouvel, Solid State Commun. 15, 441 (1974).

[14]A. R. Chowdhury, C. Allard, R. M. Suter, G. S. Collins, C. Hohenemser, and M. A. Kobeissi, Hyperfine Interact. 10, 893 (1981).

[15]J. S. Kouvel and J. B. Comly, in *Critical Phenomena in Alloys, Magnets, and Superconductors,* edited by R. E. Mills, E. Ascher, and R. I. Jaffee (McGraw-Hill, New York, 1971).

[16]A. T. Aldred and J. S. Kouvel, Physica (Utrecht) 86–88B, 329 (1977).

[17]S. J. Poon and J. Durand, Phys. Rev. B 16, 316 (1977).

[18]S. N. Kaul, Phys. Rev. B 22, 278 (1980).

[19]E. Figueroa, L. Lundgren, O. Beckman, and S. M. Bhagat, Solid State Commun. 20, 961 (1976).

[20]R. Malmhäll, G. Bäckström, K. V. Rao, S. M. Bhagat, M. Meichle, and M. B. Salamon, J. Appl. Phys. 49, 1727 (1978).

[21]K. Yamada, Y. Ishikawa, Y. Endoh, and T. Masumoto, Solid State Commun. 16, 1335 (1975).

[22]Y. Yeshurun, M. B. Salamon, K. V. Rao, and H. S. Chen, Phys. Rev. Lett. 45, 1366 (1980).

[23]T. Mizoguchi and K. Yamauchi, J. Phys. (Paris) Colloq. 35, C4-287 (1974).

[24]L. C. LeGuillou and J. Zinn-Justin, Phys. Rev. Lett. 39, 95 (1977).

[25]A. R. Arends, C. Hohenemser, and R. M. Suter, Z. Phys. B 37, 203 (1980).

[26]T. K. Bergstresser and H. Gould, J. Phys. C 12, 2611 (1979).

[27]G. S. Collins, Clark University report, 1979 (unpublished).

[28]K. W. Maring, A. J. Algra, F. Stubbe, and F. Van der Woude, J. Phys. (Paris) Colloq. 37, C6-393 (1976). For a review of hyperfine interactions in Fe alloys, see F. van der Woude and G. A. Sawatzky, Phys. Rep. 12, 335 (1974).

[29]M. A. Kobeissi and C. Hohenemser, Rev. Sci. Instrum. 49, 601 (1978).

[30]M. A. Kobeissi and C. Hohenemser, in *Magnetism and Magnetic Materials—1975 (Philadelphia),* Proceedings of the 21st Conference on Magnetism and Magnetic Materials, edited by J. J. Becker and G. H. Lander (AIP, New York, 1975), p. 497.

[31]M. A. Kobeissi, Phys. Rev. B 24, 2380 (1981).

[32]J. I. Budnick, private communication.

[33]A. Aharony, private communication.